

Accounting for biomass water equivalent variations in soil moisture retrievals from cosmic ray neutron sensor

Al-Mashharawi, Samer K.; Steele-Dunne, Susan C.; El Hajj, Marcel M.; Schrön, Martin; Doussan, Claude; Courault, Dominique; Franz, Trenton E.; McCabe, Matthew F.

DOI

[10.1016/j.agwat.2025.109493](https://doi.org/10.1016/j.agwat.2025.109493)

Publication date

2025

Document Version

Final published version

Published in

Agricultural Water Management

Citation (APA)

Al-Mashharawi, S. K., Steele-Dunne, S. C., El Hajj, M. M., Schrön, M., Doussan, C., Courault, D., Franz, T. E., & McCabe, M. F. (2025). Accounting for biomass water equivalent variations in soil moisture retrievals from cosmic ray neutron sensor. *Agricultural Water Management*, 313, Article 109493. <https://doi.org/10.1016/j.agwat.2025.109493>

Important note

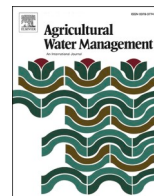
To cite this publication, please use the final published version (if applicable).
Please check the document version above.

Copyright

Other than for strictly personal use, it is not permitted to download, forward or distribute the text or part of it, without the consent of the author(s) and/or copyright holder(s), unless the work is under an open content license such as Creative Commons.

Takedown policy

Please contact us and provide details if you believe this document breaches copyrights.
We will remove access to the work immediately and investigate your claim.



Accounting for biomass water equivalent variations in soil moisture retrievals from cosmic ray neutron sensor

Samer K. Al-Mashharawi^{a,b,*}, Susan C. Steele-Dunne^b, Marcel M. El Hajj^a, Martin Schrön^c, Claude Doussan^d, Dominique Courault^d, Trenton E. Franz^e, Matthew F. McCabe^a

^a Hydrology, Agriculture and Land Observation (HALO) Laboratory, Division of Biological and Environmental Sciences and Engineering, King Abdullah University of Science and Technology (KAUST), Thuwal 23955-6900, Saudi Arabia

^b Department of Geoscience and Remote Sensing, Delft University of Technology, Delft, the Netherlands

^c Department of Monitoring and Exploration Technologies, Helmholtz Centre for Environmental Research GmbH - UFZ, Leipzig, Germany

^d INRAE, Avignon University, UMR EMMAH, F-84914, Avignon, France

^e School of Natural Resources, University of Nebraska-Lincoln, Lincoln, NE 68583, USA

ARTICLE INFO

Handling Editor Dr Z Xiyang

Keywords:

Cosmic ray neutron sensor
Biomass water equivalent
Vapor pressure deficit
Orchard
Soil moisture
Evapotranspiration

ABSTRACT

Cosmic ray neutron sensor (CRNS) has gained popularity in the last decade for its suitability in estimating area-averaged soil moisture (SM). The presence of fresh biomass influences the CRNS signal due to its water content, introducing bias to soil moisture estimation. Calibration and correction methods have been developed to account for this bias, but they usually require laborious sampling. Here, a novel approach is tested to assess the impact of biomass water equivalent (BWE) on CRNS soil moisture estimation. It was conducted in two contrasting environments from 15/11/21–1/02/23 for an olive orchard in Saudi Arabia, and from 15/02/22–30/03/23 for a cherry orchard in France. Water-uptake rates were monitored using sap flow sensors, as well as actual evapotranspiration (AET) and in-situ SM within the CRNS footprint. Concurrent environmental variables were also measured with a research-grade weather stations. It was found that when vapor pressure deficit (VPD) > 1.8kPa, CRNS-derived SM (CRNS-SM) closely matched in-situ SM measurements, which indicates minimal influence from BWE. Conversely, when VPD is lower than 1.8kPa, CRNS-SM overestimates the in-situ moisture. An optimization approach was used to find a temporally-varying value of N_0 parameter that minimizes the difference between soil moisture estimated with CRNS and in-situ sensors. Furthermore, the results showed that the relative change in the optimized value of N_0 ($N_{0,opt}$) was well correlated with VPD in both orchards ($R^2 = 0.66$ for olive and $R^2 = 0.74$ for cherry orchards), indicating a strong correlation between these variables. These findings suggest that integrating VPD and CRNS observations, and using the VPD- $N_{0,opt}$ correlation approach could be a promising way to account for the bias due to biomass dynamics on the estimation of area-averaged SM.

1. Introduction

Irrigated agriculture accounts for 40 % of global crop production. Currently, in-situ sensors such as Time-domain reflectometry (TDR) (Peters et al., 2013), tensiometers (Smajstrla and Locascio, 1996), and capacitance probes (Fares and Alva, 2000) are employed to provide precise soil moisture measurements, while sap flow measurements offer insights into tree water use in orchards (Sellami and Sifaoui, 2003). However, both approaches have limitations, including their point-scale measurement, installation and maintenance requirements, and associated costs, which restrict their practicality for commercial farms. While

microwave satellite remote sensing offers the promise of regular large-scale land observation, the spatial resolution, accuracy of data retrieval, and the requirement for validation remain a challenge for many agriculture applications (Zeng et al., 2023). Such limitations have encouraged the development of a range of novel sensors that aim to fill the gap between in-situ point-scale and satellite-based observations, while demanding less maintenance (Ochsner et al., 2013). Cosmic ray neutron sensing (CRNS) was introduced as a tool for estimating SM at the field scale, providing a means to transcend the limitations of point-scale measurements (Hydroinnova, 2017). Previous studies have demonstrated that the CRNS footprint covers up to 18 ha and sampling

* Corresponding author at: Hydrology, Agriculture and Land Observation (HALO) Laboratory, Division of Biological and Environmental Sciences and Engineering, King Abdullah University of Science and Technology (KAUST), Thuwal 23955-6900, Saudi Arabia.

E-mail address: samir.mashharawi@kaust.edu.sa (S.K. Al-Mashharawi).

<https://doi.org/10.1016/j.agwat.2025.109493>

Received 31 July 2024; Received in revised form 11 April 2025; Accepted 14 April 2025

Available online 25 April 2025

0378-3774/© 2025 The Authors. Published by Elsevier B.V. This is an open access article under the CC BY license (<http://creativecommons.org/licenses/by/4.0/>).

depths of between 0.1 and 0.8 m, depending on the soil and field characteristics (Köhli et al., 2015; Zreda et al., 2008).

CRNS has several advantages over alternative techniques used for measuring soil moisture. It is a single contactless stationary instrument, non-disruptive to field operations, and continuously provides hourly to daily data at the plot scale (Camps et al., 2016; IAEA, 2017). It consists of a neutron detector that counts the number of neutrons passing through it over a certain period within its hemispherical footprint (Köhli et al., 2015; Tan et al., 2020). The number of neutrons detected by the CRNS depends on the abundance of hydrogen atoms in the environment, due to their extraordinary efficiency in slowing down neutrons (Evelt, 2008; Zreda et al., 2008). Previous studies mainly focused on the CRNS SM product itself (Franz et al., 2015; Stevanato et al., 2019; Tan et al., 2020; Zreda et al., 2012), while vegetation water was often recognized as nuisance. However, to obtain precise SM estimations, a correction is necessary to account for all the potential pools of hydrogen within the CRNS measurement footprint (Desilets et al., 2010; Iwema et al., 2021). While correcting for hydrogen in air can be achieved using conventional measurements of air humidity from a nearby weather station (Rosolem et al., 2013), accounting for the hydrogen in the vegetation remains a challenge (Bogena et al., 2013; Franz et al., 2013), as it varies according to vegetation type, irrigation and weather conditions (Brogi et al., 2023; Li et al., 2019).

Several studies have attempted to account for the influence of vegetation cover on CRNS signals to enhance the accuracy of SM estimation (Coopersmith et al., 2014; Fersch et al., 2018; Hornbuckle et al., 2012; Jakobi et al., 2022). In particular, studies reported that the CRNS signals are sensitive to biomass water equivalent (BWE) that represents the cumulative of the vegetation water and hydrogen in the plant tissue (Franz et al., 2013). A recent long-term study for crops indicated a reduction in neutron count rate of about 1 % for every 1 kg m⁻² (or mm of water) increase in BWE (Morris et al., 2024). Generally, two types of methods have been developed for biomass corrections. The initial method involves scaling CRNS-derived SM using vegetation descriptors, such as the leaf area index. For example, Coopersmith et al. (2014) enhanced the accuracy of SM estimation from CRNS within a corn field by modeling, as a function of the leaf area index, the residuals of a linear equation between CRNS-derived SM (without considering corn effects) and in situ SM. A similar strategy was applied by Baroni and Oswald (2015) to improve CRNS-derived SM in a cropped field. The alternative method involves optimizing the calibration parameter N_0 (defined as the count rate of neutrons detected by the CRNS in a non-vegetated and dry silica soils) to account for the effects of biomass dynamics (Baatz et al., 2015; Jakobi et al., 2018; Tian et al., 2016). For instance Baatz et al. (2015) related N_0 to the BWE in kg/m², while Jakobi et al. (2018) established a relationship between N_0 and the ratio of the detected neutrons with different energy levels, known as the ratio of thermal (low energy <1 eV) to epithermal (intermediate 1 eV–10 MeV) neutrons counts during different vegetation stages. Subsequently, this method was utilized to determine optimized N_0 values throughout the growing season, leading to an improvement in CRNS-derived SM (with an error reduction of approximately 0.04 cm³/cm³). This methodology was later validated by Jakobi et al. (2022), demonstrating improved SM estimation in three different crop fields (sugar beet, winter wheat, and maize). However, Zreda et al. (2008), Andreassen et al. (2016), and Rasche et al. (2021) reported limitations of using the thermal to epithermal ratio to correct for biomass dynamics, as it is affected by soil chemistry and moisture content.

To date, the effect of BWE on CRNS signals was mainly explored in croplands where the biomass undergoes a significant change due to the fast-growing cycle (from seed to harvest) and high plant density at maturity stage. However, to our knowledge, no studies have tested the effects of BWE on CRNS signals in orchard settings, which are relatively less dense and exhibit slow biomass changes compared to annual crops. Destructive sampling methods, while accurate at individual plant level, cannot be employed to quantify the variations of BWE on a slow growing

orchard.

The objectives of this study were to test the potential of non-destructive measurements to account for the influence of BWE variations in orchards. This is needed to account for the effect of vegetation on soil moisture estimation, but could also be useful to look at water status for irrigation management including irrigation scheduling (Huang et al., 2020; Vermunt et al., 2022). To achieve this, the study aimed to use vapor pressure deficit (VPD), actual evapotranspiration (AET), and uptake rate to understand tree water dynamics and enhance the accuracy of CRNS SM estimation. The approach involved calculating AET and the uptake rate of the orchard to monitor tree water status conditions. Additionally, area-average in situ SM and CRNS SM were compared over a year. The N_0 value was dynamically adjusted to minimize the difference between CRNS and in situ SM measurements, resulting in a time series of optimized N_0 values, referred to as $N_{0,opt}$. The relative changes in $N_{0,opt}$ were compared with seasonal variations in VPD, AET, and uptake rate to argue that the variations are due to BWE and to determine if measurements of one of these quantities might be a suitable proxy to account for the effect of BWE in soil moisture retrieval.

2. Materials and methods

The study was conducted in two contrasting environments. The first was an olive orchard located in northern Saudi Arabia (desert climate) for the period from 15/11/21–1/02/23, and the second was a cherry orchard located in southeastern France (Mediterranean climate) from 15/02/22–30/03/23. CRNS sensors, sap flow meters, SM sensors, and weather stations were installed at each orchard site. Additionally, an eddy covariance system was installed in the olive orchard to measure evapotranspiration (AET) between the orchard and the atmosphere. The following paragraphs will explain each site in more detail.

2.1. Olive orchard: Al-Jouf, Saudi Arabia

Located in northern Saudi Arabia, Al-Jouf province is an arid region characterized by hot, lengthy summers and cold, dry winters. The average daily air temperature ranged from 4 °C in January to 40 °C in August, occasionally dipping below freezing in winter and exceeding 45 °C in summer (Spark, 2023). Cumulative annual rainfall does not exceed 100 mm (Al-Rashed and Sherif, 2000; El Kenawy and McCabe, 2016).

The olive orchard (*Olea europaea* "Arbequina") is a high-density grove organized into hedgerows within rectangular blocks measuring 140 × 300 m. These blocks are separated by 15-meter access roads. The planting density is 1666 trees per hectare, with the trees planted in 2010. The trees are pruned annually to maintain a height of three meters, to facilitate mechanical harvesting. The trees are spaced 1.5 m apart within rows and 4 m apart between rows (see Fig. 1a). Due to the dependence on drip irrigation, the root system concentrates within the upper soil layers. The majority of roots reach a depth between 40 and 60 cm, constituting approximately 75 % of the total root depth. A minority of roots extends vertically to depths of 1 m, while the horizontal spread reaches up to approximately a 1-meter radius around the trunk. The soil is primarily sandy, with an approximate composition of 81 % sand, 17 % silt, and the remaining 2 % consist of clay and other soil components. The trees thrive in hot, dry summers and can withstand temperatures as low as 0 °C. They typically blossom in spring (March–May), develop fruit during the summer-fall months (June–October), and undergo harvest in early winter (October–November). The period of highest water demand coincides with the summer-fall period, which corresponds to the primary growth phase of the trees.

The surface drip irrigation consists of one pipeline and two emitters per tree, as illustrated in (Fig. 1b) with an average flow rate of 2 liters per hour per dripper. Irrigation duration varies throughout the year based on the weather conditions and the farmer's crop evapotranspiration estimates. In February, it is set at 2 h every two or three days. In

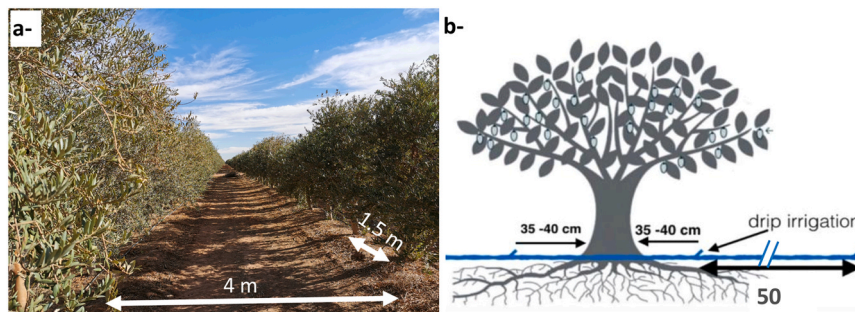


Fig. 1. Schematic of the installed drip irrigation system; and b) spacing representative of a super high density olive grove.

April, during the flowering stage, it is increased to 4 h every two days. A maximum of 7 h every second day (28 liters per tree per two days) is applied during the hottest months, July to September, which coincide with the ripening and fruit growth period. However, due to water impurities, the drippers can become partially or fully clogged and require cleaning or replacement from time to time. When the drip irrigation starts, the wet zone around the dripper undergoes a radial expansion until it reaches a stabilized radius within the range of 0.4–0.5 meters, confirmed by field measurement of multiple wet circles. Therefore, the field's soil can be categorized into dry strips and partially wet strips. The partially wet strips receive drip-irrigation that is located under the trees and have a width of approximately 1 m. Consequently, between trees (1.5 m apart), there is a 0.5-meter dry soil gap which represents one-third of the strip, meaning that within every 4 m of the field, 3 m are covered by dry soil, and one-third of the partially wet strip also remains dry. As a result, the dry portion comprises roughly 83 % of the entire area (calculated as $3/4 + 1/3 \times 1/4$), while the irrigated soil makes up the remaining 17 % of the plot.

A CRNS (CRS-2000/B, Hydroinnova LLC) was installed within the olive orchard in November 2020. The CRNS was positioned at a height of 1.5 m, aligning the top of the sensors with the canopy height of the olive trees. Additionally, an eddy covariance station, 12 SM probes installed, with 3 in-row and 3 inter-row, at varying depths 5, 20 and 40 cm (HydraProbe, Stevens Water Monitoring Systems Inc) and three sap flow meters (SFM1x, ICT International) were distributed within the footprint of the CRNS (see Fig. 2). A comprehensive gravimetric soil moisture sampling campaign was carried out on 9 November 2022 using the method as described by Desilets et al. (2010); Franz et al. (2012) to calibrate the CNRS for soil-related factors and compute N_0 . A summary of the calibration campaign, data and tree parameters are shown in Table 1 and Sections 3.1 and 3.2.

Table 1

Calibration data summary for each site and measured tree parameters for the French cherry orchard and Saudi Arabian olive orchards.

	Cherry, France		Olive, Saudi Arabia
Campaign date (dd/mm/yy)	31/05/2022	21/03/2023	09/11/2022
Average 192 SM samples measured during calibration campaign (m^3/m^3)	0.20	0.26	0.108
Soil bulk density (g/cm^3)	1.53		1.81
Total organic carbon (g/g)	0.024		0.005
Lattice water (g/g)	0.02		0.01
N_0	2838		2411
Number of trees (tree/ha)	230		1666
Tree standing volume ($m^3/tree$)	81.3		9.1
Tree density (tree/ m^2)	0.024		0.167
Average canopy dimensions (LxWxH) (m)	$5.9 \times 5.3 \times 4.0$		$2.4 \times 1.8 \times 2.7$

2.2. Cherry orchard: Entrechaux, France

The cherry orchard, is located in southeastern France within the watershed of Entrechaux town (Fig. 3). The climate in this region is Mediterranean, characterized by hot, dry summers with an average daily temperature of around 30 °C. During the winter, temperatures drop to an average daily of 10 °C (Rouault et al., 2023). The annual rainfall in this region averages between 650 and 750 mm, with the majority of the rain occurring from October to April (Funk et al., 2014). The orchard planted at a density of 240 trees per hectare and is grassed in the inter-row. To ensure a prolonged harvest season of approximately 40 days, three main cherry varieties have been planted for early, mid, and

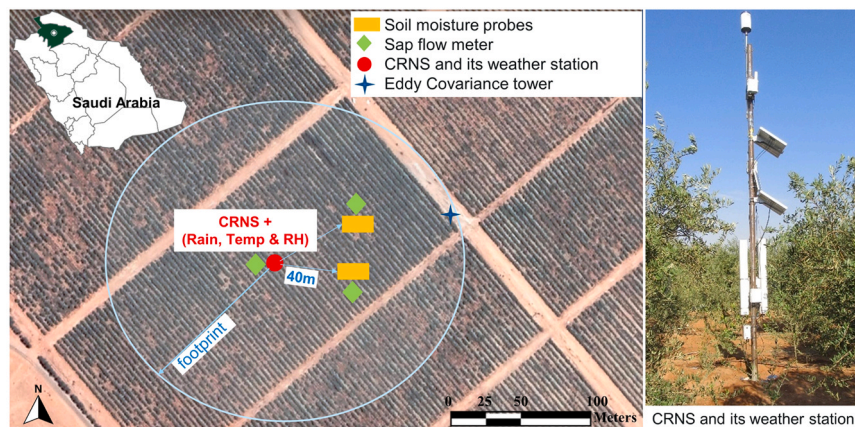


Fig. 2. The Al-Jouf olive orchard located at 29°51'39.1"N 38°19'33 and at an elevation of 635 m above sea level in Saudi Arabia. The blue circle, measuring approximately 125 m in diameter, represents the horizontal footprint of the CRNS, describing the area around the probe in which 86 % of the neutrons originate (Zreda et al., 2008).

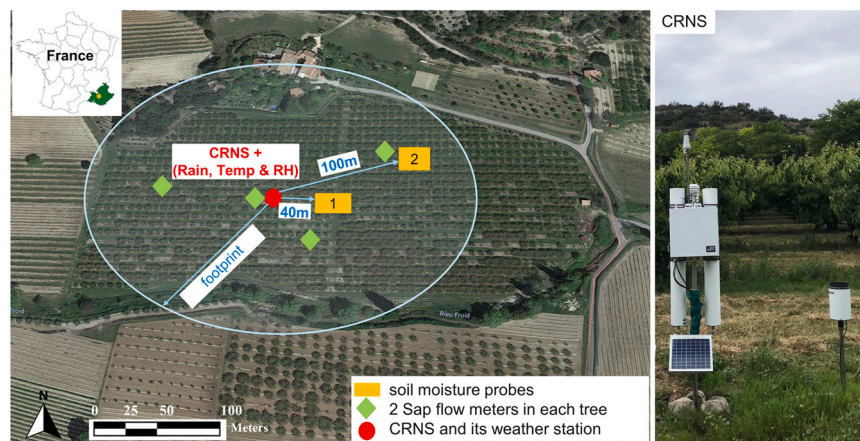


Fig. 3. The Cherry orchard site located at 44°11'34.8"N 5°09'24.1"E at an elevation of 350 m above sea level at Entrechaux, France. The blue circle represent the horizontal footprint of the CRNS and it is the area around the probe in which 86 % of the neutrons are originated (Zreda et al., 2008). A photo of the cosmic ray neutron sensor is shown on the right.

late-season yields. The orchard is equipped with a surface drip irrigation system, operating with a programmed schedule of 6 h per week in April and 3 h per day from May to mid-August. Irrigation is discontinued from mid-August onwards. The flow rate for irrigation is set at 8.2 m³/h per hectare or approximately 34.2 liters per hour per tree. According to the farmer's report, the irrigation schedule was determined based on the condition of the trees, constrained by local water management restrictions. In 2022, pruning was carried out in late November. Additionally, maintenance includes mowing of inter-row grass twice a year, specifically for 2022, it was between April 2–3 and May 27–28, followed by the natural drying of the grass in the summer. The re-greening of the inter-row grass starts from the beginning of September because of autumn rainfalls and gradually increases as the season progresses.

In February 2022, the CRNS was installed along with a standard weather station, 16 SM probes placed at different depths, spanning 5, 15, and 30 cm (HydraProbe, Stevens Water Monitoring Systems Inc) and eight sap flow meters, with two sensors installed on two branches of one tree. The distribution of all the sensors is illustrated in Fig. 3. The soil has a loamy texture with calcareous gravels. The roots of the trees may extend down to about 3 m deep. Then, two calibration field campaigns were conducted in the cherry orchard on 31 May 2022 and 21 March 2023 (Table 1). During each campaign, volumetric sampling for calibration was carried out to calculate N_0 (Section 3.2) using the method as described by Desilets et al. (2010); Franz et al. (2012).

In addition to soil sampling, various tree dimensions, including tree height, canopy length, and width, were measured for over 100 trees in a rectangular-wave pattern to cover a larger representative area at both the cherry and olive orchards. A summary of the tree parameters for both of these sites is presented in Table 1, which highlights key differences in tree densities, average canopy dimensions and above-ground standing volume.

2.3. In-situ soil moisture measurements

Continuous reference in-situ SM measurements in each orchard field were obtained by averaging data from in situ SM sensors installed at the olive and cherry sites. The sensors were divided into two groups positioned at distances of 40 and 100 m from the CRNS, represented by the orange rectangles in Figs. 2 and 3. Each group was further subdivided into two sets. The first was positioned along the tree rows at depths of 5, 15, and 30 cm, this set represents 17 % of the field area because it is subjected to irrigation. While the second set was installed at the same depth distribution but placed between the rows of trees (inter-rows) and this set represents 83 % of the field which remains non-irrigated. Of course, neutron counts have a stronger correlation with SM in the upper

soil layers than in the deeper zones, and their relationship varies with distance. Hence, it is not applicable to simply average SM data from sensors at different depths for direct comparison with CRNS-SM estimates. To address these spatial and depth-related variations, we employed a physical approach outlined by Schrön et al. (2017), which factors sensor depth and distance from the CRNS. Schrön et al. (2017), method involved assigning a weighting coefficient between 0 and 1 to each SM value at various depths and distance and summing the weighted values, allowed us to obtain representative weighted averaged in situ SM data for comparison with CRNS-SM estimates.

2.4. Water uptake rate measurements

Sap flow meters are used to continuously measure tree water uptake rates in both small woody stems as well as in large trees. Sap flow meters are stand-alone instruments that have been widely used to provide insight into irrigation management and transpiration rates (El Hajj et al., 2022; Puig-Sirera et al., 2021; Sun et al., 2022). The system used in both fields is SFM1 from ICT international Pty Ltd, which uses the principle of Heat Ratio Method to measure high, low and reverse flow rates in liters per hour (l/hr) (Burgess et al., 2001; Marshall, 1958). Each device consists of three needles (Fig. 4b), where the middle needle acts as a heating pulsation and the upper and lower needles contain outer and inner thermistors (Fig. 4a). As per the manufacturer recommendations, needles inserted such that the outer thermistor is 2.5 mm inside the sapwood (Fig. 4c). A flat blade screwdriver was turned horizontally and hammered into the barkwood of stem until it stops moving which indicates the beginning of sap wood. If the bark is thinner than 10 mm, a small spacer was used so that the outer measurement point stays within 2.5 mm in the outer sapwood. After installing the needles, they were isolated and protected from environmental conditions such as dust, rain and radiation.

The trees selected for sap flow meter installation in both fields are located away from the edges of the plot and had similar characteristics

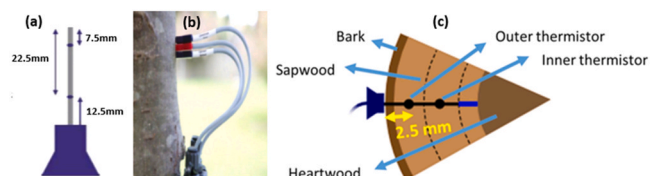


Fig. 4. (a) location of thermistors within the SFM1 needle set. (b) Sap flow meter needles installed in a tree trunk. (c) Sketch of a needle inside the main trunk.

as the majority of the surrounding olive or cherry trees in terms of height and canopy dimensions and age to ensure representative measurements. For the olive trees, 6 SFMs were installed, each on a main trunk of a tree (Fig. 5a) with each device installed approximately 50 cm from the soil surface. For the cherry trees, the main trunk had been treated with a sticky pesticide coating. Therefore, two SFMs were installed on two representative branches from each tree, so that a total of 8 SFMs were installed on four trees (Fig. 4b). Thus, for each field, it was assumed that the measured water-uptake rate of the selected trees was similar to the majority of trees within that field. For olive orchards, the uptake rate from all six SFMs were averaged to represent the flow rate within the CRNS footprint. For the cherry trees, the total flow rate of each of the four trees was determined by taking the average of the two SFMs and multiplying it by the number of branches. The collected water uptake data were processed 10-min intervals using the Sap Flow Tool software (ICT International Pty. Ltd). Finally, the total flow rate value was divided by the tree density from Table 1, to convert the flow rate from liter per hour per tree (l/hr/tree) into a rate per unit area, expressed in millimeters per day per square meter (mm/day).

3. Data and methods

3.1. Neutron counts correction factors

To retrieve soil moisture from neutron counts, there is a calibration process that begins by considering factors that influence the neutron counts. These include the sensor's location, elevation, atmospheric pressure, atmospheric water vapor, and incoming neutron flux intensity, and have been considered in previous studies. Eq. (1) shows how to calculate the corrected neutron count rates:

$$N = N' * f_p * f_v * f_i \begin{cases} f_p = \exp\left(\frac{(P - P_{ref})}{\beta}\right) \\ f_v = 1 + \alpha(v - v_{ref}) \\ f_i = \frac{N_{ref}}{N_i(t)} \end{cases} \quad (1)$$

where N is the corrected neutron counts per hour (cph), N' is the raw moderated neutron counts (cph), f_p is the pressure correction factor (Zreda et al., 2012), f_v is the water vapor correction factor (Rosolem et al., 2013), f_i is the neutron intensity correction factor (Zreda et al., 2012). In f_p , P is the current ambient pressure (mb), P_{ref} is the reference pressure (mb), and β is the attenuation length of neutrons (g/cm^2) in specific location. In f_i , $N_i(t)$ is the current high-energy neutron intensity, N_{ref} is the reference high-energy neutron intensity. In f_v , v is the absolute

humidity of the air (g/m^3), v_{ref} is the reference absolute humidity of the air (g/m^3), α is humidity reference = 0.0054.

3.2. Calibration function and converting neutrons into soil moisture estimate

After the correction factors, the following calibration function proposed by (Desilets et al., 2010) using the software tool cornish pasdy (https://git.ufz.de/CRNS/cornish_pasdy) model version 0.8 was applied to convert neutron count into water content Eq. (2):

$$\theta_{total} = \theta_p + \theta_{lw} + \theta_{soc} + \theta_{bwe} = \frac{0.0808}{\frac{N}{N_0} - 0.372} - 0.115 \quad (2)$$

where θ_{total} is the total water content (g/g), which consists of all hydrogen sources in the soil, θ_p is gravimetric soil water content (g/g), θ_{lw} is lattice water content (g/g), θ_{soc} is soil organic carbon water content (g/g), θ_{bwe} biomass water equivalent (g/g). N represents the corrected epithermal fast neutron counts in counts per hour (cph), corrected as described in Section 3.1. N_0 represents the theoretical count rate of neutrons detected by the CRNS in a non-vegetated field with dry silica soils within the instrument footprint. The fitted constants a_0 , a_1 , and a_2 have values of 0.0808, 0.372, and 0.115, respectively, which are applicable for most soil types (Desilets et al., 2010).

To compute N_0 , we used a rearranged form of Eq. (2) and carried out a comprehensive gravimetric SM sampling campaign in order to obtain θ_p on that day. Following the sampling framework proposed by Franz (2012). Our approach involved more intensive sampling in closer proximity to the CRNS, recognizing the heightened influence of SM within the first 30 m of the CRNS (Köhli et al., 2015). The soil samples were collected from 32 locations with six samples from each location at varying depths: 0–5, 5–10, 10–15, 15–20, 20–25 and 25–30 cm (resulting in a total of 192 samples). The sampling structure consists of five radial distances (R) ranging from 10 to 200 m from the CRNS probe. Specifically, radial distance of 10 m (R10) comprised 12 sampling sites with 30° intervals, followed by R50 with six sites at 60° intervals, R100 with six sites at 60° intervals, R150 with four sites at 90° intervals and R200 with four sites at 90° intervals. To preserve moisture content, the collected samples were sealed in aluminum cans and their fresh wet weight were measured on-site. Subsequently, these samples underwent oven drying at 105°C for a duration of 72 h, after which their dry weights were determined in the laboratory.

Eight soil samples were selected for the lattice and soil organic carbon (SOC) analysis from the pool of the soil samples collected for gravimetric SM measurement for both sites. One sample was selected from each radial distance, and mixed samples were created by combining soil from various random locations. First, all the soil samples were crushed using ball mill grinder (PM200, Retsch) for proper sample mixing and size reduction of the soil particles. For soil organic carbon (θ_{soc}) determination, the total weight (g) of each sample was measured, then HCl was added to eliminate inorganic carbon (IC). Subsequently, the samples were kept at 65°C overnight to ensure the completion of the reaction and sample dryness. Then, an elemental analyzer (Flash 2000 CHNS/O, Thermo Fisher Scientific) was used to determine the total concentration of carbon (TC) by combustion processes up to 1000°C . The total soil organic carbon (TOC) is the subtraction between the total carbon (TC) and the inorganic carbon (TIC). Then to convert TOC into water equivalent in (g/g), we used the following equation:

$$\theta_{soc} = (TC - TIC) * 1.724 * f_{we} \quad (3)$$

where 1.724 is a constant to convert total organic carbon into total organic matter, and $f_{we} = 0.494$ is the stoichiometric ratio of H_2O to organic carbon (Franz et al., 2015). In the case of lattice water analysis (θ_{lw}), a thermogravimetric analyzer (TG 209 F1 Iris, Netzsch) was used with a controlled temperature at 150°C , during which the samples were observed for phase transition over time at certain temperature values.

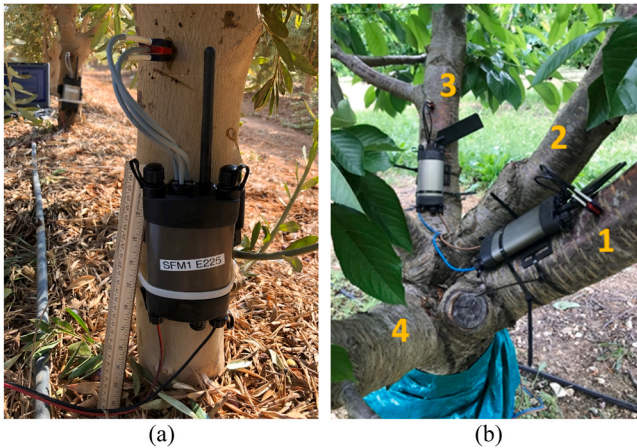


Fig. 5. (a) sap flow meter (SFM) installed on the main trunk of an olive tree. (b) Two SFMs installed in two branches of a cherry orchard that consists of 5 main branches.

The lattice water content was measured as a percentage of the total sample weight, which was then divided by 100 to obtain the value in g/g. Note that a biomass water equivalent of $\theta_{bwe} = 0$ g/g was considered in Eq. (2). Its influence will be incorporated in the revised calibration equation instead, which will be an outcome of this study (Section 3.5).

3.3. Actual evapotranspiration (AET) measurements

For the olive orchards, an eddy covariance station (Li-7500A, Li-Cor Inc., USA) was installed at the edge of the field at a height of approximately 4.5 m. The setup includes a 3D sonic anemometer (WindMaster Pro, Gill Instruments Limited, UK) for measuring wind speed in three directions and an open-path infrared gas analyzer for measuring water vapor and CO₂ concentration. It also contains meteorological sensors that provide data on air temperature, humidity, net radiation, and rainfall. The collected flux data were processed using EddyPro software (Version 7.0.9) to generate 30-min averaged AET flux measurements. Further information about this station, along with data processing and energy balance enclosure, was detailed in a previous publication co-authored by myself and colleagues (Elfarkh et al., 2023).

In such high-density orchards in an arid climate, it is expected that transpiration predominates in the total AET. The two primary water sources are the drip irrigation system and the water within the olive trees, with the surrounding soil being dry and bare. The drip irrigation system delivers water directly to the root zone, and the dense canopy shades the dripper spots, which restricts the evaporation (Moriani et al., 2003). In such arid conditions, the high atmospheric demand for moisture drives higher transpiration rates. Olive trees, known for their adaptability to such conditions, maximize the use of available water for transpiration (Goldhamer et al., 2006; Luque et al., 2006). Therefore, in these conditions, it is reasonable to estimate that transpiration could account for around 80–90 % of the total AET, while evaporation would constitute about 10–20 %.

For the cherry orchard, there was no eddy covariance tower but a weather station was installed about 40 m away from the CRNS on the same tree's row. This station included a net radiometer (NR Lite2, KIPP and ZONEN) temperature and relative humidity sensor (HMP155, Vaisala), wind speed and direction sensors (2D windSonic, Gill instrument) and a tipping bucket rain gauge. Reference evapotranspiration (ET_0) was estimated using the FAO-56 Penman-Monteith approach described by Allen et al. (1998).

A widely used approach to derive maximal actual evapotranspiration (AET) from reference ET_0 involves using a single crop coefficient (K_c) described in FAO56 (Allen et al., 1998). The K_c values were adjusted throughout the growing season of the cherry orchard as reported by Liegeois (2024) for this region, to ensure accurate AET estimation as shown in Eq. (4):

$$AET = K_c ET_0 \quad (4)$$

For the initial stage (early spring to pre-bloom, February 15 to March 30), $K_{c,ini}$ was set at 0.6. During the mid-season (bloom to early fruit development, March 30 to June 10), $K_{c,mid}$ increased to 0.7. In the late stage (fruit ripening to post-harvest, June 10 to July 15), $K_{c,end}$ was adjusted to 0.5, and for the remaining periods, it was set to 0.4. Further details are provided in the results section and illustrated in Figs. 7 and 8

3.4. Vapor pressure deficit

Vapor pressure deficit (VPD) is the difference between the amount of moisture in the air and the maximum amount of moisture in the air at saturation level at a particular temperature. In plants, it is used to describe the difference in water vapor pressure between the inside of a leaf and the surrounding air. Grossiord et al. (2020) suggested that VPD can be a useful indicator of biomass water equivalent. Therefore, the higher the VPD, the higher atmospheric evaporative stress (Franks et al.,

1997). Multiple studies have found that in forest trees, high VPD increased trees water losses through transpiration and tree water content reached its lowest during the summer, when VPD levels peaked (Flo et al., 2022; Jamshidi et al., 2021). As recent studies in olive orchards (El Hajj et al., 2023) have shown that VPD and water uptake rate are correlated. VPD was calculated using the relative humidity and temperature data that are co-located with the CRNS station using Eq. (5) below:

$$VPD = e_s(1 - R_h/100) \quad (5)$$

Where, e_s is the saturation vapor pressure which can be calculated from the air temperature, R_h is the relative humidity (Allen et al., 1998).

3.5. Measuring the impact of biomass water equivalent on neutron counts

The impact of BWE on neutron counts has been identified in previous research (Baatz et al., 2015; Franz et al., 2015; Hawdon et al., 2014). Baatz et al. (2015) has found a correlation between the calibration factor N_0 and BWE. In order to be able to include BWE value in N_0 calculation across different growth stages, multiple calibration campaigns including vegetation sampling would be needed. These are time-consuming, costly and labor-intensive. Therefore, it is difficult to perform this calibration with the frequency needed to account for the BWE variations. As an alternative, an optimization approach was used to find a temporally-varying value of N_0 that minimizes the difference between soil moisture estimated with CRNS and in-situ sensors. A value of N_0 is found for every 10-day interval, and the time series in N_0 was compared to uptake rate, AET and VPD to see if the variations are related to BWE. The soil moisture estimated with this time-varying N_0 will be referred to as CRNS-SM _{N_0,opt}

Then a time series of the percentage deviation from the initial N_0 values was calculated by taking the difference between $N_{0,opt}$ values and the initial N_0 value using Eq. (6):

$$\% \text{ deviation} \in N_0 = 100 - \left(\frac{N_{0,opt}}{N_0} \right) * 100 \quad (6)$$

4. Results

4.1. Weighted average in-situ soil moisture

Fig. 6 illustrates the average in-situ SM values at each depth and the total depth weighted average SM for both the olive (Fig. 6a) and cherry (Fig. 6b) orchards, respectively. In the olive orchard, an obvious daily fluctuation in SM data is evident in the sensors positioned beneath the trees, reflecting the effects of daily irrigation. Due to the arid nature of the region, irrigation is quickly followed by a rapid decline in SM as the water is quickly transpired. In contrast, probes situated between the rows (inter-rows) within the same area, show minimal influence from irrigation, confirming that the wetted soil volumes are confined to the immediate vicinity around the drippers. The weighted average SM values are closer to inter-row SM due to the higher assigned weight (0.83) for inter-row SM in comparison to in-row SM. In the cherry orchard, the weighted average SM (depicted by the black line) is higher than that in the olive orchard. The impact of multiple rainfall events throughout the year (primarily occurring from November to January) is evident in the cherry orchard data, whereas the olive orchard experiences fewer rain events. The weighted average in-situ SM will serve as the reference against which CRNS-estimated SM will be compared in the following sections.

4.2. Effects of biomass water equivalent on neutron counts derived soil moisture

Fig. 7a shows CRNS-SM estimates, using a single N_0 value obtained during the calibration campaign, and the weighted average in situ SM in

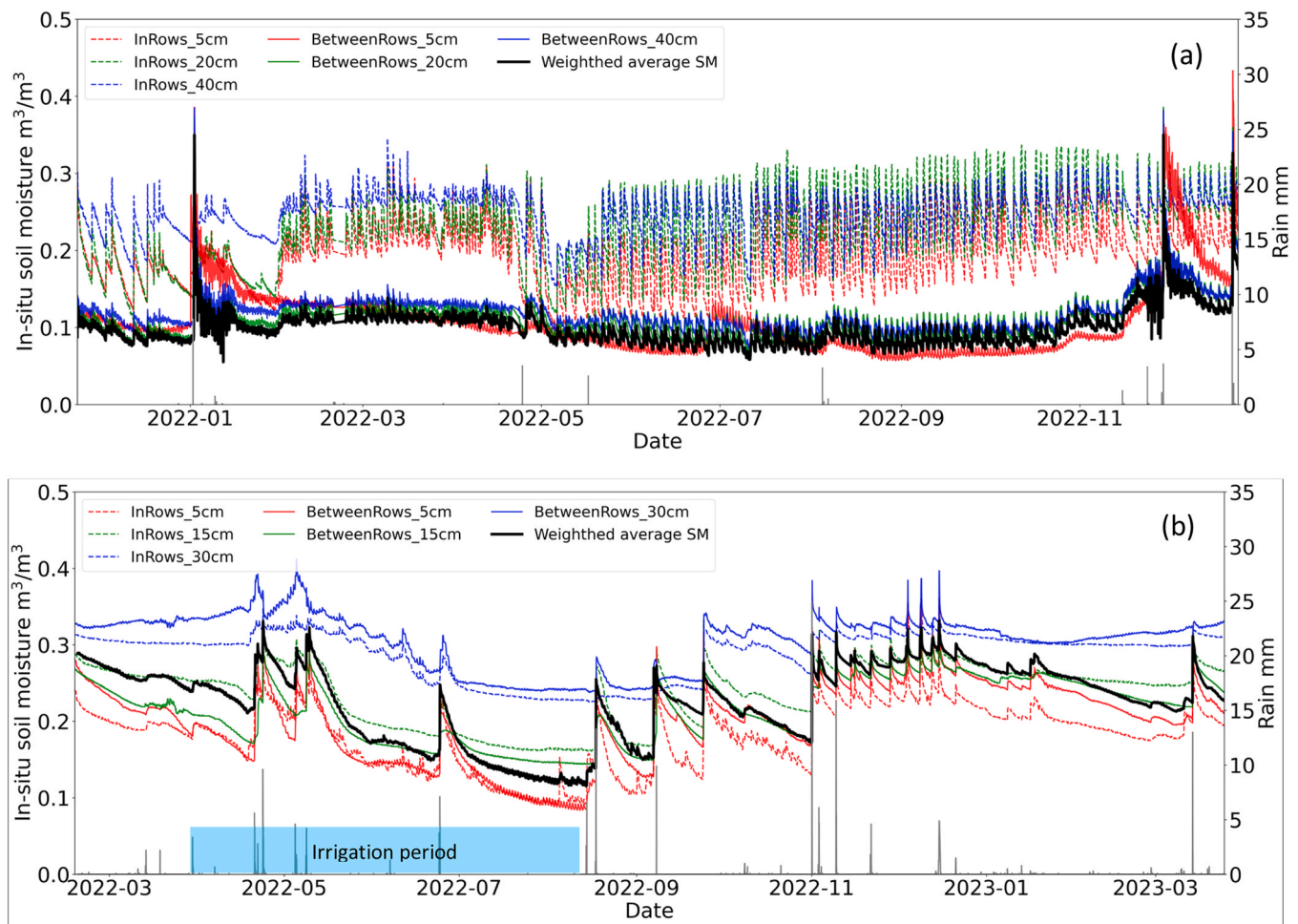


Fig. 6. Time series of in-situ SM at the (a) olive orchard and (b) cherry orchard. The dashed and continuous lines represent the average in-row and inter-rows SM values, respectively. The black line shows the weighted average in situ SM for all the sensor data.

the olive orchard. To reduce noise, a Savitzky-Golay filter (windows = 12 h) was applied to smooth CRNS-derived SM (Davies et al., 2022; Franz et al., 2020). The results indicate that throughout the year, the CRNS-derived SM values are overestimated compared to the weighted average SM particularly in autumn and winter during the dormancy and flowering period with mean difference of $\pm 0.03 \text{ m}^3/\text{m}^3$ (average error = 28 %), then agrees well during the fruit growth, ripening and harvest period between May and November with mean difference of $0.005 \text{ m}^3/\text{m}^3$ (average error percent = 10 %) (Fig. 7a). Overestimation suggests the presence of an additional source of hydrogen beyond that of SM between January and May and after November. An overestimation is observed at rainfall events due to interception, which increases the water content (hydrogen pool) within the CRNS footprint and leads to a sudden false increase in the estimated SM (Baroni and Oswald, 2015).

Similarly, the long-term overestimation observed during cooler periods (from January to May and after November) can be attributed to the effect of vegetation water content. During these cooler periods, the daily average temperature falls below 10°C , and vapor pressure deficit values are below 1.8 kPa (as shown in Fig. 7b). In addition, the actual evapotranspiration (AET) and uptake rate are generally low and the values are close to each other (Fig. 7c). These factors indicate that the trees are not transpiring significantly and the water content is stable within the trees. Furthermore, the olive trees enter a dormant phase (Fig. 7b), during which they internally store nutrients and water to sustain themselves through this period (Rallo et al., 1994). These combined factors contribute to greater neutron storage by the trees, and consequently to an overestimation of SM from the CRNS. Conversely, during warmer

periods (between May and November), with daily irrigation, it can be observed that actual evapotranspiration, which is 80–90 % transpiration, is generally higher than the uptake rate. This is shown by the negative values of uptake rate minus AET in Fig. 7c. This difference reaches its maximum when VPD values are high ($>1.8 \text{ kPa}$), indicating that the transpiration rate exceeds the daily uptake rate. Consequently, the BWE is reduced to a level where its contribution to the CRNS counts is minimal. This minimal contribution results in CRNS SM estimates closely matching the reference SM.

In the cherry orchard (Fig. 8), similar results were observed, with high VPD values combined with AET values above the uptake rate level, indicating a decrease in BWE, leading to a closer SM estimation. The CRNS-derived SM overestimated reference SM during periods of low VPD ($<1.8 \text{ kPa}$) from February to July (dormancy, flowering, and fruit set period) with a mean difference of $0.06 \text{ m}^3/\text{m}^3$ (average error = 25 %). Similarly, from September to March of the next year (the second dormancy period), it had a mean difference of $0.09 \text{ m}^3/\text{m}^3$ (average error = 35 %). In contrast, it matched reference SM during high VPD conditions with a mean difference of $0.003 \text{ m}^3/\text{m}^3$ (average error = 2.4 %) (Fig. 8a, b). There was a VPD spike from June 15 to June 23, 2022, where VPD increased from 1 kPa to 2 kPa, leading to agreement between estimated and reference SM.

Moreover, when irrigation stopped during the harvest (June – July), the uptake rate declined rapidly, resulting in large negative values of uptake rate minus AET in Fig. 8c. During this time, with VPD values above 1.8 kPa, a match between reference and estimated SM due to the reduced contribution from BWE was observed. In an unpublished study

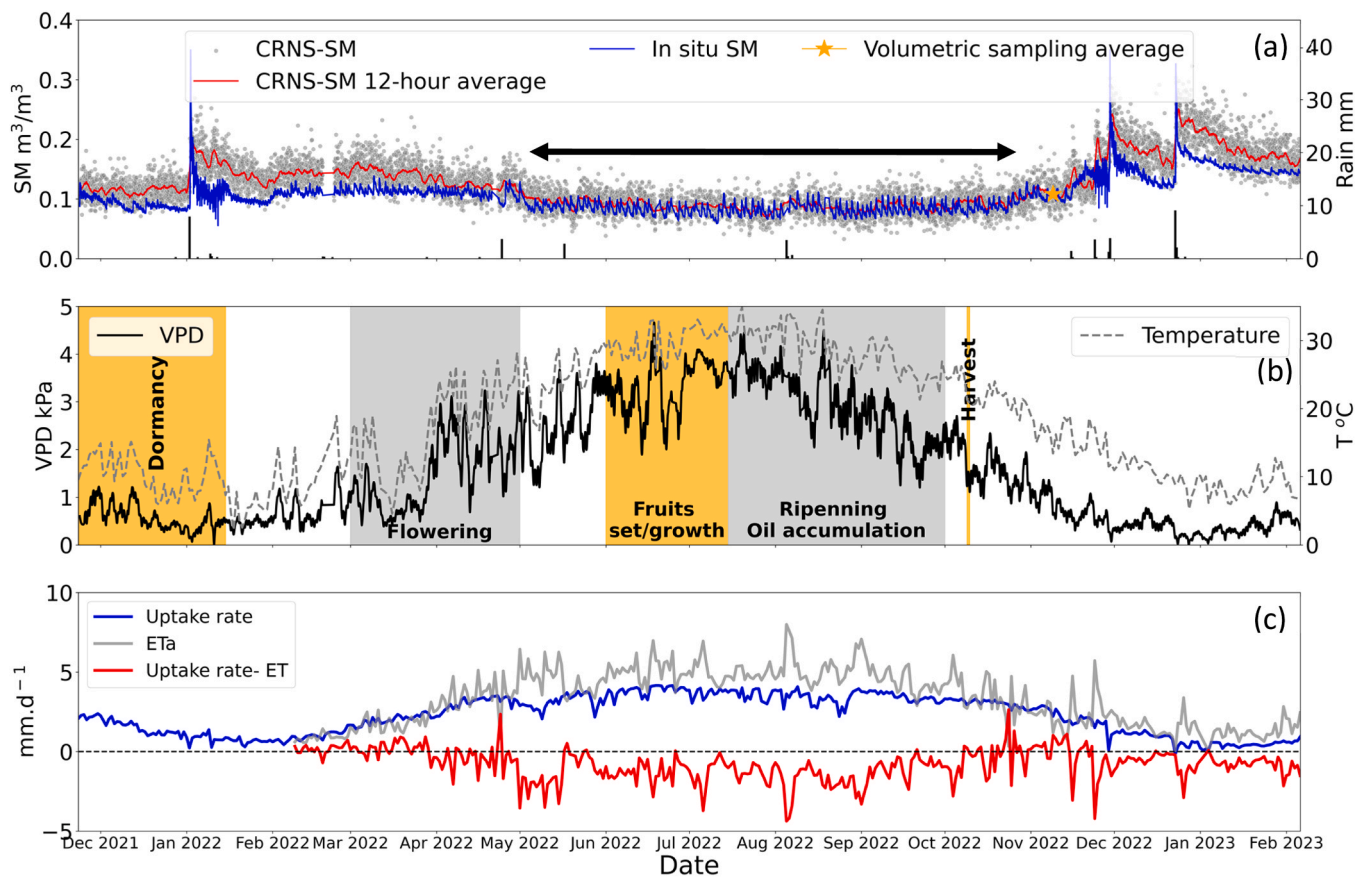


Fig. 7. Olive orchard - (a) in-situ and CRNS-derived SM. The black double arrow in (a) highlight the period (May–Nov) during which CRNS-derived SM aligns with the in-situ SM. and (b) vapor pressure deficit and temperature data. (c) Shows uptake rates from sap.

on the same site, a SM profile analysis estimated the water content in the 0–50 cm soil layer. The study found that during July and August, the water amount fell below the readily available water stock (80 mm), causing tree water stress during this period (Personal communication Doussan C, EMMAH INRAE Avignon). This finding supports our conclusion that the close correspondence between CRNS-derived SM and in situ SM is attributed to a decrease in BWE, and is supported by high VPD values. Starting from September, a series of rain events reduced VPD and increased root zone soil moisture and regrowth of the inter-row grass, resulting in overestimation of CRNS SM.

The results presented in Fig. 7 and Fig. 8 demonstrate that using a single value of N_0 obtained from the calibration campaign, resulted in an error in estimated CRNS-SM $_{N_0}$ that is related to changes in BWE. Figs. 9 (a) and 10(a) show that using a time series of optimized N_0 to produce CRNS-SM $_{N_0, opt}$ values (black line), instead of the single N_0 value (red line) reduced the error between the CRNS SM and the in situ SM measurements (blue line). In addition, the cherry orchard showed greater changes in N_0 values, with a 320 cph difference between the maximum and minimum N_0 values (i.e., 2770–3090 cph) shown in Figs. 9(b) and 10(b). This variation is due to more distinct seasonal changes in BWE for cherry trees during different phenological stages, as well as higher uptake rate variations during the irrigation periods. In contrast, the olive orchard exhibited a smaller range of 150 cph, with a minimum N_0 of 2270 cph and a maximum N_0 of 2420 cph. Most importantly, the change in N_0 was found to co-vary with seasonal changes in VPD, AET, and uptake rate values at both sites.

The relationship between the percentage of change in N_0 and VPD, AET and uptake rate was analyzed for each site over an entire year of data (Fig. 11). Results show a consistent relationship between the change in N_0 and VPD across the different orchard environments with good correlation ($R^2 \sim 0.7$). When VPD exceeds 1.8 kPa, the drop in N_0

remains constant, indicating that no effects of BWE beyond VPD > 1.8 kPa. This finding suggests that VPD may be useful to estimate the impact of BWE on the CRNS neutron counts for orchard environments. VPD is particularly valuable because it is easy to estimate using temperature and humidity data that is generally available alongside the CRNS for atmospheric correction. In addition, it is a non-destructive method with high temporal resolution.

Fig. 11 also shows the relationship between the change in N_0 in relation to actual evapotranspiration and uptake rate for olive and cherry orchards. For the olive orchard, the results show a strong and positive relationship with both AET and uptake rate, leading to high correlation coefficients ($R^2 = 0.71$ and 0.74 , respectively). Conversely, for the cherry orchard, the relationship is relatively weak ($R^2 = 0.51$ and 0.23 for AET and uptake rate, respectively).

In the desert climate of the olive orchard, the study site consists of bare soil, trees, and drip irrigation, with minimal rain events. As a result, any parameter related to tree water content whether directly such as AET and uptake rate or indirectly such as VPD showed a strong correlation with BWE and, therefore, with N_0 values. In this dry environment, the water held in the vegetation is the primary hydrogen pool and any variation in water storage (e.g. a change in AET or uptake rate) will have a significant effect on N_0, opt .

On the other hand, in the cherry orchard with a Mediterranean climate, with frequent rain events and relatively lower VPD values, the presence of inter-row grass increases AET at certain times of the year, as seen in Fig. 8(c). Additionally, the rain affect the ratio of evaporation to transpiration in the AET values, leading to a low correlation between AET and N_0 values. Moreover, the water content in the trees remains more stable since AET closely matches the uptake rate for most of the year, except during periods of rain or active inter-row grass growth (Hirasawa et al., 1987). Therefore, the weak relationship observed for

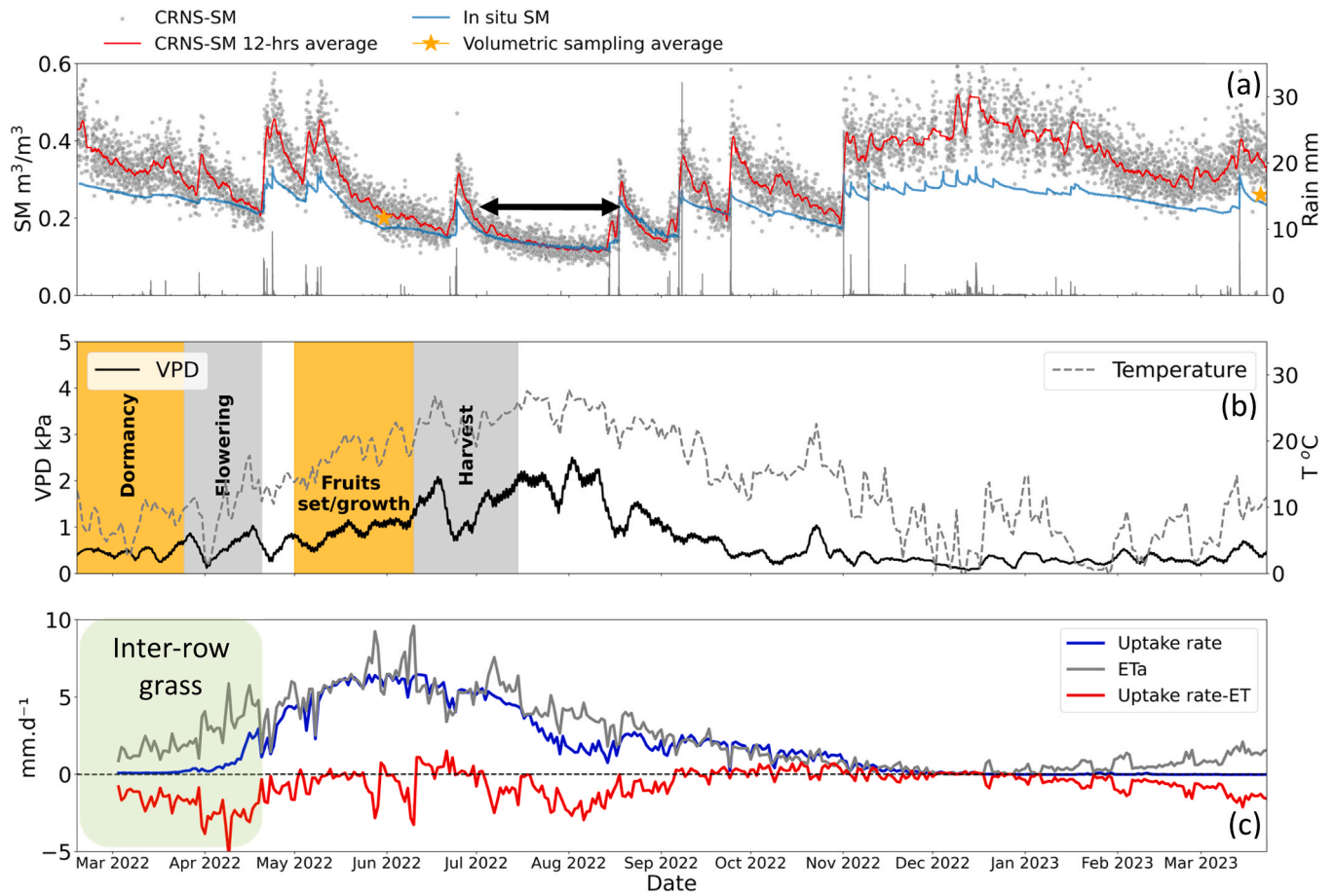


Fig. 8. Cherry orchard - (a) in-situ and CRNS-derived SM, (b) vapor pressure deficit and temperature data and the phenological stages of the cherry orchard (c) shows uptake rates, AET and BWE (uptake rate minus AET).

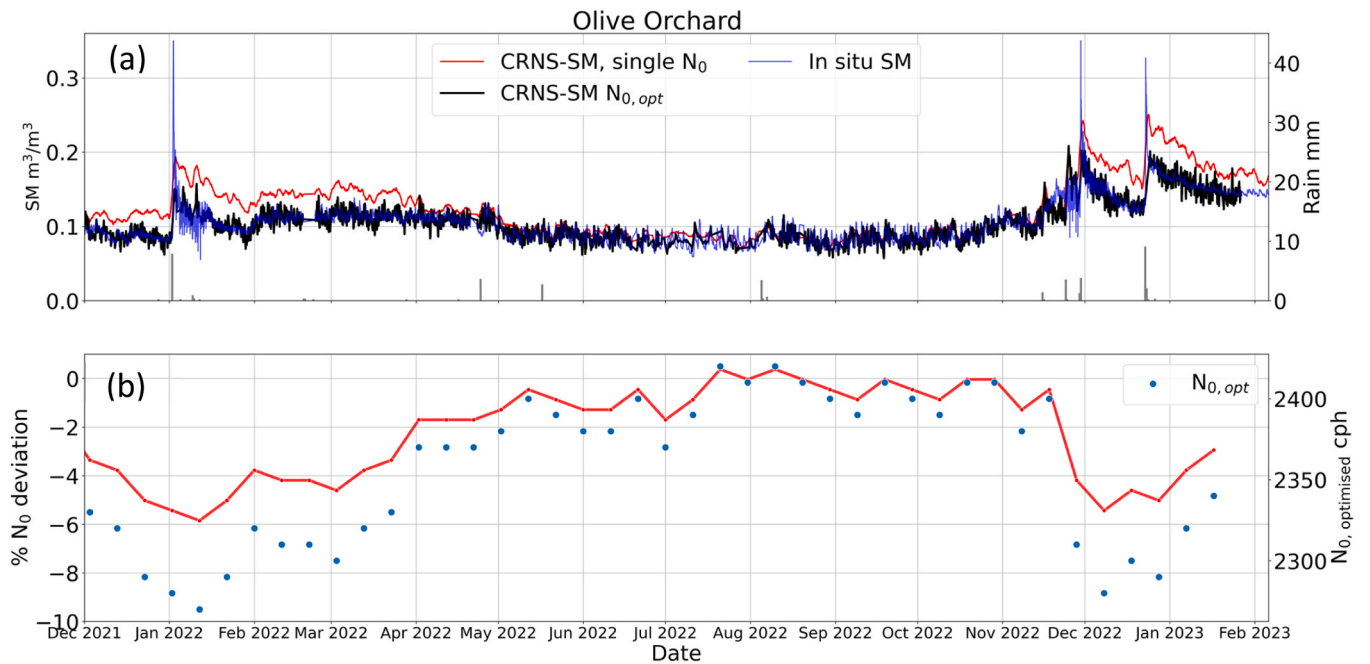


Fig. 9. (a) The red line represents the CRNS SM estimation using reference N_0 value obtained from the calibration campaign (see Table 1). The black line shows the CRNS SM using optimized N_0 values, while the blue line represents the reference in-situ weighted average SM data. (b) Shows the percentage change in N_0 value and the corresponding N_0 value.

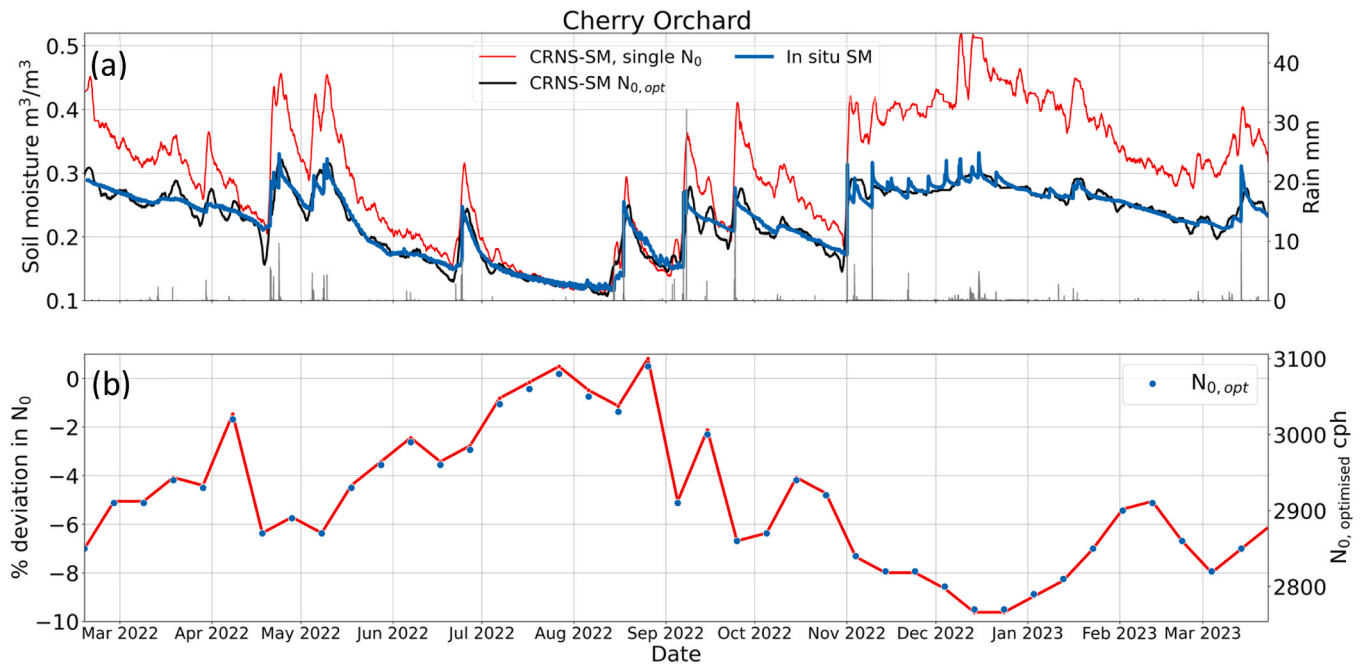


Fig. 10. (a) Red line represents the CRNS SM estimation using N_0 value from Table 1. The black line shows the CRNS SM using optimized N_0 values, while the blue line represents reference in-situ weighted average SM data. (b) shows change in N_0 value.

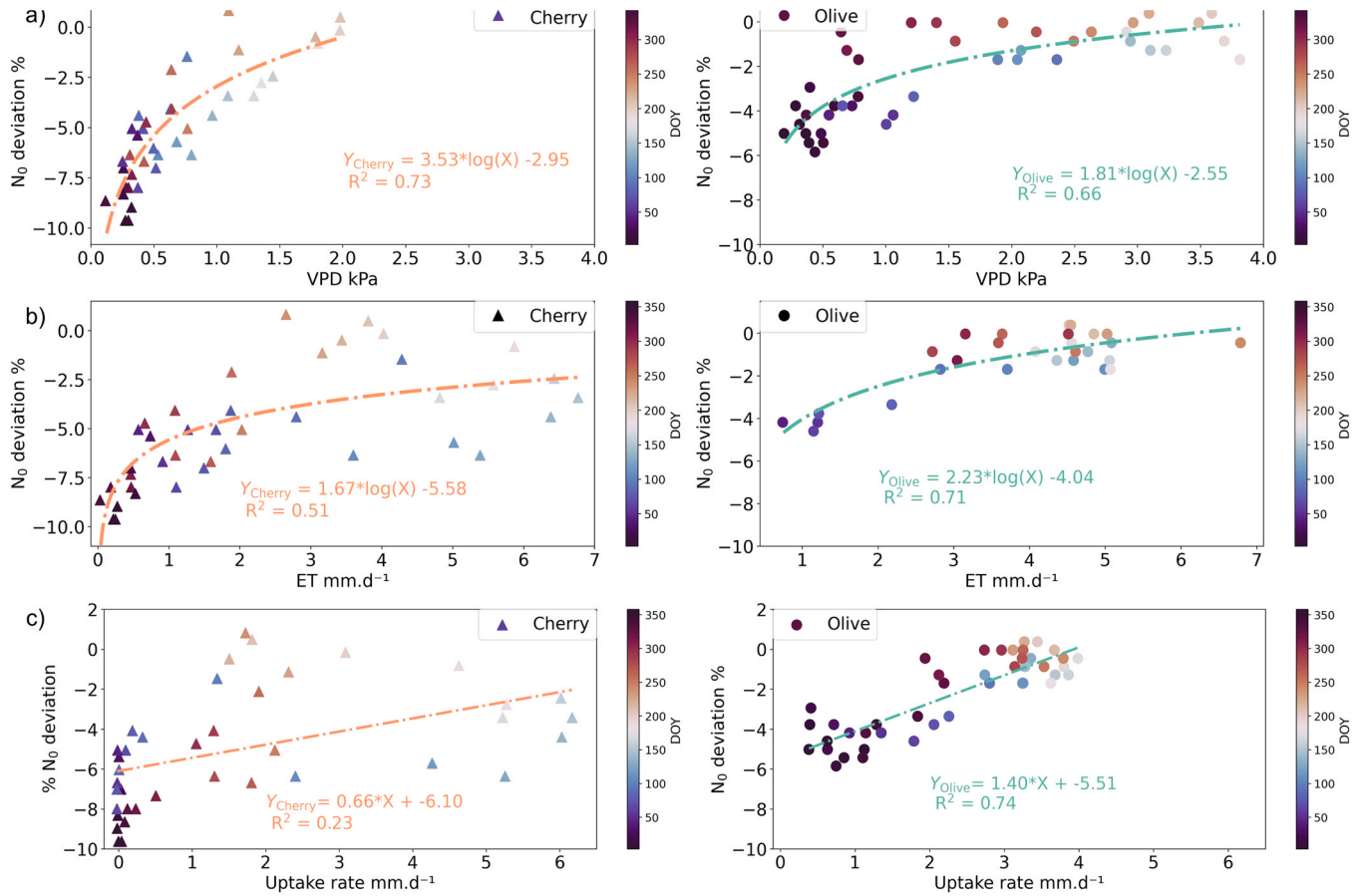


Fig. 11. The natural logarithmic correlation between the change in N_0 and: a) VPD and b) AET over a full year of data for the cherry and olive orchards. c) The linear correlation between daily uptake rate and change in N_0 over the full year period.

the cherry orchard suggests that variations in the daily water uptake rate have less impact on tree water content itself.

5. Discussion

In this study, inconsistencies were expected between CRNS-derived SM and in situ SM (mainly over-estimations). These inconsistencies arose due to observed seasonal variations in BWE, consequently affecting the hydrogen pool within the CRNS footprint in response to dry and wet weather conditions. It was assumed that this inconsistency would be at its minimum during the summer, as the amount of hydrogen in the trees would be at its lowest due to high transpiration rates and temperature. In contrast, during the winter (characterized by lower temperatures and reduced transpiration), the inconsistency was expected to be the highest, resulting in an overestimation of reference SM. This overestimation occurs because of an increased hydrogen pool within the trees, leading to reduced neutron counts and, consequently, an overestimation of SM.

VPD from a weather station, uptake rate from sap flow meters and AET measurements were used to explore the effect of BWE on neutron counts in two different orchards settings. The obtained results confirms that there is an effect of BWE on CRNS neutron counts which causes a difference in SM estimation with the in situ measurements that can reach up to 35 %. This aligns with conclusions from previous studies conducted in crop fields and forest. Importantly, this study shows that VPD has more potential than the uptake rate and AET to correct biomass water effects on neutron counts. The results showed that $N_{0,opt}$ values were well correlated with the VPD ($R^2 \sim 0.7$), and this correlation was consistent in both study sites, despite differing climates, species and phenological development.

VPD is calculated from relative humidity (RH) and temperature (T), and these two parameters were already used for CRNS atmospheric correction. However, VPD, along with AET and uptake rate, was used to infer BWE dynamics. In other words, neither VPD, uptake rate, nor AET can directly measure water storage volume within the tree itself, as tree water content is determined by the difference between the root uptake rate and transpiration rate (Grossiord et al., 2020). For example, if the tree is full of water and the root zone is depleted, then a period of high VPD and uptake rate would lead to gradual decrease in BWE. However, when both the tree and root zone are dry, then changes in VPD will not influence BWE because the plant will remain dry. Therefore, VPD is not a direct proxy for BWE, as the relationship between the two depends on vegetation and climate conditions. Nonetheless, VPD can provide insight into the influence of atmospheric demand driving changes in BWE.

Previous studies reported that a drop of 1 % in N_0 corresponds to an estimated biomass density of approximately 1 kg/m^2 (or 1 mm) of biomass water equivalent change (Baatz et al., 2015; Franz et al., 2015; Morris et al., 2024). In this study, a maximum drop in N_0 of 4 % and 9.5 % (Fig. 11) was required to correct for biomass effects on CRNS-derived SM in the olive and cherry field, respectively. These maximum percentages were observed at the early and late stages of the growing season (dormancy), when the tree starts accumulating water (increase of BWE) within its internal structures, preparing for the demands of various physiological processes such as leaf development, flower blossoming, and fruit formation. These drops in N_0 suggest that BWE yearly variations is up to 4 kg/m^2 in the olive field, and up to 9.5 kg/m^2 in the cherry field. The larger BWE dynamic for the cherry field compared to the olive is because the cherry trees have substantially larger above-ground biomass and greater dimensions compared to the olive trees allowing to store more water (refer to Table 1).

The results showed no significant change in the neutron counts at harvest time in the olive and orchard fields. In the olive fields, harvesting was carried out in one day on October 10 2022 using a machine harvester. According to the farmer's laboratory analysis, the yield was 4.8 t/ha , with 57 % of the olives being water, or 0.27 kg/m^2 , which would translate to about 0.27 % drop in N_0 value. Given this, it is not

expected to have a significant impact on the neutron counts. For the cherry orchards, it was expected that there would be a minimal effect of harvesting on neutron count, given that hand harvesting took place over a 40 days period. Therefore, from Fig. 7-a, the discrepancy between measured and estimated SM decreases from beginning of harvest to the end. Indeed VPD also increased, but an effect of the decrease of water in fruits on the better estimation of SM could also be possible.

Future studies should explore the accuracy of estimating BWE based on the drop of N_0 , as obtained in this study for different vegetated areas with existing in situ SM sensors. Validation of CRNS-derived BWE accuracy requires in situ destructive sampling, which could be inapplicable for trees. A possible solution for sampling over trees is to use thermal sensors on board of Unmanned Aerial Vehicle (Marsal and Girona, 2017).

6. Conclusion

The aim of this study was to investigate the impact of biomass water equivalent (BWE) on neutron counts and explore correction methods. AET and uptake rate were used to identify periods of reduced tree water content by detecting the times when transpiration exceeds uptake rates. Additionally, vapor pressure deficit (VPD), AET, and uptake rate served as indicators of BWE effects on CRNS counts. To assess the influence of BWE on neutron counts, we compared in situ SM measurements with CRNS-estimated SM. Seasonal differences between in situ and CRNS-estimated SM, along with variations in VPD confirmed their correlation with changes in BWE.

The results showed that changes in N_0 values correlates strongly with VPD, with $R^2 \approx 0.70$ for both sites, suggesting that incorporating VPD into CRNS calibration could improve soil moisture accuracy. Uptake rate showed a high correlation with N_0 in the olive orchard ($R^2 = 0.73$), but a weaker relation $R^2 = 0.23$ in the cherry orchard. In this case, the variability was attributed to differences in tree species and distinct weather conditions. For example, in olive trees during periods of high evaporative demand, transpiration exceeds the uptake rate, resulting in a gradual reduction in tree water content (i.e. lower BWE). In contrast, in the cherry orchard, irrigation practices lead to the uptake rate matching the transpiration rate, allowing trees to keep the water content level stable. Regarding AET, strong correlations were found in the olive orchard, whereas in the cherry orchard, the presence of inter-row grass increases AET during certain times of the year. Additionally, rain affected the evaporation to transpiration ratio in AET values, resulting in a weaker correlation between AET and N_0 values.

The findings highlights the significance of understanding how biomass water content affects CRNS signals. Data from additional sites are needed to evaluate whether the VPD can be used as a parameter to improve SM estimation from CRNS sensor across a diverse range of climatic and vegetation conditions.

CRedit authorship contribution statement

Courault Dominique: Writing – review & editing, Visualization, Validation, Supervision, Data curation. **Franz Trenton E:** Writing – review & editing, Validation, Resources, Methodology, Investigation, Conceptualization. **McCabe Matthew F.:** Writing – review & editing, Validation, Supervision, Methodology, Funding acquisition, Conceptualization. **El Hajj Marcel M.:** Writing – review & editing, Visualization, Software. **Schrön Martin:** Software, Methodology, Investigation. **Doussan Claude:** Writing – review & editing, Validation, Supervision, Resources, Data curation. **Al-Mashharawi Samer K:** Writing – original draft, Methodology, Conceptualization. **Steele-Dunne Susan C.:** Writing – review & editing, Visualization, Supervision, Project administration, Investigation.

Declaration of Competing Interest

The authors declare that they have no known competing financial interests or personal relationships that could have appeared to influence the work reported in this paper.

Acknowledgment

The funding for this research was supported by the King Abdullah University of Science and Technology. Authors would like to express their gratitude to the team at INRAE, Avignon in France and Al-Jouf Agricultural Company (JADCO) in Saudi Arabia for their support and assistance during the installation and calibration of sensors in the field campaigns. We also acknowledge the Analytical Core Lab at King Abdullah University of Science and Technology (<https://corelabs.kaust.edu.sa/>) for providing the essential facilities and resources necessary for the chemical analytical procedures carried out in this study.

Data availability

Data will be made available on request.

References

- Allen, R.G., Pereira, L.S., Raes, D. and Smith, M., 1998. Crop evapotranspiration—Guidelines for computing crop water requirements—FAO Irrigation and drainage paper 56. Fao, Rome, 300(9): D05109.
- Al-Rashed, M.F., Sherif, M.M., 2000. Water resources in the GCC countries: an overview. *Water Resour. Manag.* 14 (1), 59–75.
- Andreasen, M., et al., 2016. Modeling cosmic ray neutron field measurements. *Water Resour. Res.* 52 (8), 6451–6471.
- Baatz, R., et al., 2015. An empirical vegetation correction for soil water content quantification using cosmic ray probes. *Water Resour. Res.* 51 (4), 2030–2046.
- Baroni, G., Oswald, S.E., 2015. A scaling approach for the assessment of biomass changes and rainfall interception using cosmic-ray neutron sensing. *J. Hydrol.* 525, 264–276.
- Bogena, H.R., Huisman, J.A., Baatz, R., Hendricks Franssen, H.-J., Vereecken, H., 2013. Accuracy of the cosmic-ray soil water content probe in humid forest ecosystems: the worst case scenario. *Water Resour. Res.* 49 (9), 5778–5791.
- Broggi, C., et al., 2023. Monitoring irrigation in small orchards with cosmic-ray neutron sensors. *Sensors* 23 (5), 2378.
- Burgess, S.S.O., et al., 2001. An improved heat pulse method to measure low and reverse rates of sap flow in woody plants. *Tree Physiol.* 21 (9), 589–598.
- Camps, A., et al., 2016. Sensitivity of GNSS-R spaceborne observations to soil moisture and vegetation. *IEEE J. Sel. Top. Appl. Earth Obs. Remote Sens.* 9 (10), 4730–4742.
- Coopersmith, E.J., Cosh, M.H., Daughtry, C.S.T., 2014. Field-scale moisture estimates using COSMOS sensors: A validation study with temporary networks and leaf-area indices. *J. Hydrol.* 519, 637–643.
- Davies, P., Baatz, R., Bogena, H.R., Quansah, E., Amekudzi, L.K., 2022. Optimal temporal filtering of the cosmic-ray neutron signal to reduce soil moisture uncertainty. *Sensors* 22 (23), 9143.
- Desilets, D., Zreda, M., Ferré, T.P.A., 2010. Nature's neutron probe: land surface hydrology at an elusive scale with cosmic rays. *Water Resour. Res.* 46.
- El Hajj, M.M., Almarsharawi, S.K., Johansen, K., Elfarkh, J., McCabe, M.F., 2022. Exploring the use of synthetic aperture radar data for irrigation management in super high-density olive orchards. *Int. J. Appl. Earth Obs. Geoinf.* 112, 102878.
- El Hajj, M.M., Johansen, K., Almarsharawi, S.K., McCabe, M.F., 2023. Water uptake rates over olive orchards using sentinel-1 synthetic aperture radar data. *Agric. Water Manag.* 288, 108462.
- El Kenawy, A.M., McCabe, M.F., 2016. A multi-decadal assessment of the performance of gauge- and model-based rainfall products over Saudi Arabia: climatology, anomalies and trends. *Int. J. Climatol.* 36 (2), 656–674.
- Elfarkh, J., Johansen, K., El Hajj, M.M., Almarsharawi, S.K., McCabe, M.F., 2023. Evapotranspiration, gross primary productivity and water use efficiency over a high-density olive orchard using ground and satellite based data. *Agric. Water Manag.* 287, 108423.
- Evert, S., 2008. A Practical Guide to Methods Instrumentation and Sensor Technology, Field Estimation of Soil Water Content. INTERNATIONAL ATOMIC ENERGY AGENCY, Vienna, pp. 39–41.
- Fares, A., Alva, A.K., 2000. Evaluation of capacitance probes for optimal irrigation of citrus through soil moisture monitoring in an entisol profile. *Irrig. Sci.* 19 (2), 57–64.
- Fersch, B., Jagdhuber, T., Schrön, M., Völksch, I., Jäger, M., 2018. Synergies for soil moisture retrieval across scales from airborne polarimetric SAR, cosmic ray neutron roving, and an in situ sensor network. *Water Resour. Res.* 54 (11), 9364–9383.
- Flo, V., Martínez-Vilalta, J., Granda, V., Mencuccini, M., Poyatos, R., 2022. Vapour pressure deficit is the main driver of tree canopy conductance across biomes. *Agric. For. Meteorol.* 322, 109029.
- Franks, P.J., Cowan, I.R., Farquhar, G.D., 1997. The apparent feedforward response of stomata to air vapour pressure deficit: information revealed by different experimental procedures with two rainforest trees. *Plant, Cell Environ.* 20 (1), 142–145.
- Franz, T.E., et al., 2012. Measurement depth of the cosmic ray soil moisture probe affected by hydrogen from various sources. *Water Resour. Res.* 48 (8).
- Franz, T., 2012. Installation and calibration of the cosmic-ray solar moisture probe, University of Arizona.
- Franz, T.E., et al., 2013. Ecosystem-scale measurements of biomass water using cosmic ray neutrons. *Geophys. Res. Lett.* 40 (15), 3929–3933.
- Franz, T.E., et al., 2020. Practical data products from cosmic-ray neutron sensing for hydrological applications. *Front. Water* 2 (9).
- Franz, T.E., Wang, T., Avery, W., Finkenbinder, C., Brocca, L., 2015. Combined analysis of soil moisture measurements from roving and fixed cosmic ray neutron probes for multiscale real-time monitoring. *Geophys. Res. Lett.* 42 (9), 3389–3396.
- Funk, C.C. et al., 2014. A quasi-global precipitation time series for drought monitoring. 832, Reston, VA.
- Goldammer, D.A., Viveros, M., Salinas, M., 2006. Regulated deficit irrigation in almonds: effects of variations in applied water and stress timing on yield and yield components. *Irrig. Sci.* 24 (2), 101–114.
- Grossiord, C., et al., 2020. Plant responses to rising vapor pressure deficit. *N. Phytol.* 226 (6), 1550–1566.
- Hawdon, A., McJannet, D., Wallace, J., 2014. Calibration and correction procedures for cosmic-ray neutron soil moisture probes located across Australia. *Water Resour. Res.* 50 (6), 5029–5043.
- Hirasawa, T., ARAKI, T., ISHIHARA, K., 1987. The relationship between water uptake and transpiration rates in rice plants. *Jpn. J. Crop Sci.* 56 (1), 38–43.
- Hornbuckle, B., Irvin, S., Franz, T., Rosolem, R. and Zweck, C., 2012. The potential of the COSMOS network to be a source of new soil moisture information for SMOS and SMAP, 2012 IEEE International Geoscience and Remote Sensing Symposium, pp. 1243–1246.
- Huang, Y., Ren, Z., Li, D., Liu, X., 2020. Phenotypic techniques and applications in fruit trees: a review. *Plant Methods* 16 (1), 107.
- Hydroinnova, 2017. Hydroinnova's soil moisture and snow sensors have burgeoning impact on hydrological sciences.
- IAEA, 2017. International atomic energy agency: Cosmic Ray Neutron Sensing: Use, Calibration and Validation for Soil Moisture Estimation. INTERNATIONAL ATOMIC ENERGY AGENCY, Vienna.
- Iwema, J., Schrön, M., Koltermann Da Silva, J., Schweiser De Paiva Lopes, R., Rosolem, R., 2021. Accuracy and precision of the cosmic-ray neutron sensor for soil moisture estimation at humid environments. *Hydrol. Process.* 35 (11), e14419.
- Jakobi, J., Huisman, J.A., Fuchs, H., Vereecken, H., Bogena, H.R., 2022. Potential of thermal neutrons to correct cosmic-ray neutron soil moisture content measurements for dynamic biomass effects. *Water Resour. Res.* 58 (8), e2022WR031972.
- Jakobi, J., Huisman, J.A., Vereecken, H., Dieckkrüger, B., Bogena, H.R., 2018. Cosmic ray neutron sensing for simultaneous soil water content and biomass quantification in drought conditions. *Water Resour. Res.* 54 (10), 7383–7402.
- Jamshidi, S., Zand-Parsa, S., Niyogi, D., 2021. Assessing crop water stress index of citrus using in-situ measurements, landsat, and sentinel-2 data. *Int. J. Remote Sens.* 42 (5), 1893–1916.
- Köhli, M., et al., 2015. Footprint characteristics revised for field-scale soil moisture monitoring with cosmic-ray neutrons. *Water Resour. Res.* 51 (7), 5772–5790.
- Li, D., et al., 2019. Can drip irrigation be scheduled with cosmic-ray neutron sensing? *Vadose Zone J.* 18 (1), 190053.
- Liegeois, B., 2024. Memento Irrigation, France.
- Luque, J.E.F., et al., 2006. Water relations and gas exchange in olive trees under regulated deficit irrigation and partial rootzone drying. *Springer Nature*.
- Marsal, J. and Girona, J., 2017. VIII International Symposium on Irrigation of Horticultural Crops, Lleida, Spain. *Acta Horticulturae*(1150).
- Marshall, D.C., 1958. Measurement of sap flow in conifers by heat transport. 1. *Plant Physiol.* 33 (6), 385–396.
- Moriana, A., Orgaz, F., Pastor, M., Fereres, E., 2003. Yield responses of a mature olive orchard to water deficits. *J. Am. Soc. Hortic. Sci.* 128 (3), 425–431.
- Morris, T.C., Franz, T.E., Becker, S.M., Suyker, A.E., 2024. Effect of biomass water dynamics in cosmic-ray neutron sensor observations: a long-term analysis of maize-soybean rotation in Nebraska. *Sensors* 24 (13), 4094.
- Ochsner, T.E., et al., 2013. State of the art in large-scale soil moisture monitoring. *Soil Sci. Soc. Am. J.* 77 (6), 1888–1919.
- Peters, R.T., Desta, K.G., Nelson, L., 2013. Pract. Use Soil moisture Sens. their data Irrig. Sched.
- Puig-Sirera, À., et al., 2021. Transpiration and water use of an irrigated traditional olive grove with sap-flow observations and the FAO56 dual crop coefficient approach. *Water* 13 (18), 2466.
- Rallo, L., Torreño, P., Vargas, A., Alvarado, J., 1994. Dormancy and alternate bearing in olive. *Int. Soc. Hortic. Sci.* 127–136.
- Rasche, D., Köhli, M., Schrön, M., Blume, T., Güntner, A., 2021. Towards disentangling heterogeneous soil moisture patterns in cosmic-ray neutron sensor footprints. *Hydrol. Earth Syst. Sci.* 25 (12), 6547–6566.
- Rosolem, R., et al., 2013. The effect of atmospheric water vapor on neutron count in the cosmic-ray soil moisture observing system. *J. Hydrometeorol.* 14 (5), 1659–1671.
- Rouault, P. et al., 2023. Using High Spatial Resolution Satellite Imagery for Improved Agricultural Management of Mediterranean Orchards. *Social Science Research Network (SSRN)*.
- Schrön, M., et al., 2017. Improving calibration and validation of cosmic-ray neutron sensors in the light of spatial sensitivity. *Hydrol. Earth Syst. Sci.* 21 (10), 5009–5030.
- Sellami, M.H., Sifaoui, M.S., 2003. Estimating transpiration in an intercropping system: measuring sap flow inside the oasis. *Agric. Water Manag.* 59 (3), 191–204.

- Smajstrla, G.A., Locascio, J.S., 1996. Tensiometer-controlled, drip-irrigation Scheduling of tomato. *Appl. Eng. Agric.* 12 (3), 315–319.
- Spark, W., 2023. Weather History at Al-Jawf Domestic Airport. <https://shorturl.at/opFJZ>.
- Stevanato, L., et al., 2019. A novel cosmic-ray neutron sensor for soil moisture estimation over large areas. *Agriculture* 9 (9), 202.
- Sun, X., Li, J., Cameron, D., Moore, G., 2022. On the use of sap flow measurements to assess the water requirements of three Australian native tree species. *Agronomy* 12 (1), 52.
- Tan, X., et al., 2020. Applicability of cosmic-ray neutron sensor for measuring soil moisture at the agricultural-pastoral ecotone in northwest China. *Sci. China Earth Sci.* 63 (11), 1730–1744.
- Tian, Z., Li, Z., Liu, G., Li, B., Ren, T., 2016. Soil water content determination with cosmic-ray neutron sensor: correcting aboveground hydrogen effects with thermal/fast neutron ratio. *J. Hydrol.* 540, 923–933.
- Vermunt, P.C., Steele-Dunne, S.C., Khabbazan, S., Judge, J., van de Giesen, N.C., 2022. Extrapolating continuous vegetation water content to understand sub-daily backscatter variations. *Hydrol. Earth Syst. Sci.* 26 (5), 1223–1241.
- Zeng, J., Peng, J., Zhao, W., Ma, C., Ma, H., 2023. Microwave remote sensing of soil moisture. *Remote Sens.* 15 (17), 4243.
- Zreda, M., et al., 2012. COSMOS: the cosmic-ray soil moisture observing system. *Hydrol. Earth Syst. Sci.* 16 (11), 4079–4099.
- Zreda, M., Desilets, D., Ferré, T.P.A., Scott, R.L., 2008. Measuring soil moisture content non-invasively at intermediate spatial scale using cosmic-ray neutrons. *Geophys. Res. Lett.* 35 (21).